Large-scale calculations of the double-β decay of ^{76}Ge, ^{130}Te, ^{136}Xe, and ^{150}Nd in the deformed self-consistent Skyrme quasiparticle random-phase approximation

M. T. Mustonen[1,2,*] and J. Engel[1,†]

[1]*Department of Physics and Astronomy, CB 3255, University of North Carolina, Chapel Hill, North Carolina 27599-3255, USA*

[2]*Department of Physics, Central Michigan University, Mount Pleasant, Michigan 48859, USA*

(Received 29 January 2013; revised manuscript received 8 May 2013; published 5 June 2013)

We use the axially deformed Skyrme quasiparticle random-phase approximation (QRPA) together with the SkM* energy-density functional, both as originally presented and with the time-odd part adjusted to reproduce the Gamow-Teller resonance energy in ^{208}Pb, to calculate the matrix elements that govern the neutrinoless double-β decay of ^{76}Ge, ^{130}Te, ^{136}Xe, and ^{150}Nd. Our matrix elements in ^{130}Te and ^{136}Xe are significantly smaller than those of previous QRPA calculations, primarily because of the difference in pairing or deformation between the initial and the final nuclei. In ^{76}Ge and ^{150}Nd, our results are similar to those of less computationally intensive QRPA calculations. We suspect the ^{76}Ge result, however, because we are forced to use a spherical ground state, even though our mean-field theory indicates a deformed minimum.

DOI: 10.1103/PhysRevC.87.064302 PACS number(s): 21.60.Jz, 23.40.Hc

I. INTRODUCTION

Neutrinoless ($0\nu\beta\beta$) double-β decay can occur if neutrinos are Majorana particles at a rate that depends on a weighted average of neutrino masses (see Refs. [1,2] for reviews). The experimental search for $0\nu\beta\beta$ is approaching sensitivity to neutrino masses below 100 meV [3]. To extract a mass from the results, however, or to set a reliable upper limit, will require accurate values of the nuclear matrix elements that govern the decay, matrix elements that cannot be measured and must, therefore, be calculated. A number of theorists have attempted the calculations by applying several distinct methods. Among the most popular is the proton-neutron quasiparticle random phase approximation (QRPA).

The QRPA can be carried out at various levels of sophistication. So far, with only a few exceptions [4–9], the mean fields on which the QRPA is based have been spherical by fiat; most of those that allow deformation have restricted themselves to single-β decay or two-neutrino double-β ($2\nu\beta\beta$) decay. And although many employ a kind of self-consistent QRPA [10–12], only Ref. [13] has carried out the QRPA without the use of an artificially inert core, and there, again, the calculation (which was relativistic) was restricted to $2\nu\beta\beta$ decay. In none of the calculations has the residual QRPA interaction ever been fully consistent with that of an underlying Hartree-Fock-Bogoliubov (HFB) calculation. Finally, even Ref. [13], which treats all the nucleons as active, forces them to occupy harmonic-oscillator levels rather than continuumlike states. Here, we overcome all these limitations by allowing axially symmetric deformation, by using a modern and well-tested Skyrme functional for both the HFB mean-field calculation and the QRPA that is based on it, by keeping all the nucleons active, and by placing the nucleus inside a large cylindrical box so that discretized versions of continuum states are available up to high energy.

In recent years, deformed Skyrme-QRPA calculations of this type have been applied extensively to nuclear vibrations (see, e.g., Refs. [14–18]) and will soon be applied to single-β decay [19]. Our implementation, described in detail below, is via a B-spline-based HFB code with the above-mentioned cylindrical-box boundary conditions, followed by the construction and diagonalization of the QRPA Hamiltonian matrix in the basis of canonical two-quasiparticle states. The calculations consume enough CPU hours to require a supercomputer, and so we restrict ourselves to four isotopes—^{76}Ge, ^{130}Te, ^{136}Xe, and ^{150}Nd—used in the some of the most promising current or proposed experiments [20–28]. The deformation and pairing in the initial and final nuclei are often quite different, and matrix elements can be suppressed as a result [5]; our numbers depend crucially on the overlap of intermediate-nucleus states created by exciting the initial ground state with those created by exciting the final ground state. The QRPA supplies only transition amplitudes and so must be extended to obtain the overlap. Here, we will apply a prescription like that in Ref. [5] while noting that a well-justified and tractable expression is still lacking.

This article is organized as follows: Sec. II contains a brief overview of the matrix elements that govern double-β decay and of the Skyrme QRPA. Section III describes the details of our computational implementation, and Sec. IV presents our results. Section V is a conclusion.

II. DOUBLE-β DECAY AND THE QRPA

A. Decay operators

The lifetime for $0\nu\beta\beta$ decay, if there are no heavy particles that mediate the decay, is

$$\left[T^{0\nu}_{1/2}\right]^{-1} = G'^{0\nu}\langle m_\nu\rangle^2 |M'^{0\nu}|^2, \tag{1}$$

where $\langle m_\nu\rangle^2$ is a weighted average of three neutrino masses, $G'^{0\nu}$ is a phase-space factor (recently recomputed in Ref. [29]),

*mika.t.mustonen@unc.edu
†engelj@physics.unc.edu

and $M'^{0\nu}$ is a nuclear matrix element.[1] Although the matrix element contains intermediate states and an energy denominator, it can, to good approximation [31], be represented by one that involves only the initial and final ground states. In this "closure" approximation and by neglecting the small tensor term, one can write the matrix element as

$$M'^{0\nu} = \frac{2R}{\pi(1.25)^2}\int_0^\infty q\,dq \times \langle f|\sum_{a,b}\frac{j_0(qr_{ab})[h_F(q)+h_{\rm GT}(q)\vec{\sigma}_a\cdot\vec{\sigma}_b]}{q+\bar{E}-(E_i+E_f)/2}\tau_a^+\tau_b^+|i\rangle, \quad (2)$$

where the factor 1.25 is inserted by convention, $|i\rangle$ and $|f\rangle$ are the ground states of the initial and final nuclei, $r_{ab}=|\vec{r}_a-\vec{r}_b|$ is the distance between nucleons a and b, j_0 is the usual spherical Bessel function, $\bar{E}$ is an average excitation energy to which the matrix element is insensitive (and for which we use the value 10 MeV), and the nuclear radius $R\equiv 1.2A^{1/3}$ fm is inserted with a compensating factor in the phase-space function to make the matrix element dimensionless. The "form factors" h_F and $h_{\rm GT}$ are given by

$$\begin{aligned} h_F(q) &\equiv -g_V^2(q^2),\\ h_{\rm GT}(q) &\equiv g_A^2(q^2)-\frac{g_A(q^2)g_P(q^2)q^2}{3m_p}\\ &\quad+\frac{g_P^2(q^2)q^4}{12m_p^2}+\frac{g_M^2(q^2)q^2}{6m_p^2}, \end{aligned} \quad (3)$$

with

$$\begin{aligned} g_V(q^2) &= \frac{1}{[1+q^2/(0.71\ {\rm GeV}^2)]^2},\\ g_A(q^2) &= \frac{1.27}{[1+q^2/(1.09\ {\rm GeV}^2)]^2},\\ g_P(q^2) &= \frac{2m_p g_A(q^2)}{q^2+m_\pi^2}, \quad g_M(q^2)=3.70g_V(q^2). \end{aligned} \quad (4)$$

Here, m_p and m_π are the proton and pion masses.

The two-neutrino double-β decay rate, which we will use to fit parameters for our $0\nu\beta\beta$ calculation, can be written as

$$\left[T_{1/2}^{2\nu}\right]^{-1} = G^{2\nu}|M^{2\nu}|^2, \quad (5)$$

where $G^{2\nu}$ is another phase-space factor (also recomputed in Ref. [29]) and $M^{2\nu}$ is a matrix element. The closure approximation is not good for two-neutrino decay, and the matrix element must contain intermediate states explicitly,

$$M^{2\nu} \approx \sum_n \frac{\langle f|\sum_a \vec{\sigma}_a\tau_a^+|n\rangle\langle n|\sum_b\vec{\sigma}_b\tau_b^+|i\rangle}{E_n-(M_i+M_f)/2}, \quad (6)$$

where n labels states in the intermediate nucleus with energy E_n, M_i and M_f are the masses of initial and final nuclei, and the effects we have neglected—forbidden currents, the Fermi matrix element, etc.—are small [32–34].

Recent studies [35,36] have shown that realistic short-range correlations have only a small effect on the double-β matrix elements. To include them here, even approximately, would complicate our computational procedure considerably, and so we omit them altogether.

B. Deformed charge-changing QRPA

The self-consistent axially symmetric Skyrme-HFB-QRPA method for like-particle excitations, on which our code is based, is described thoroughly in Refs. [14,15,37]. We modify the code discussed there in a rather straightforward way to work with charge-changing modes rather than like-particle modes. Obviously, we must change the basis of like-two-quasiparticle states to a basis of one-quasiproton–one-quasineutron states. We then construct the QRPA matrix given in Eqs. (A1)–(A6) of Ref. [37] with the following changes: (a) We remove the Coulomb interaction, and (b) we keep only the terms in the effective particle-hole Skyrme interaction—displayed in Eq. (B13) of Ref. [37]—that contribute to the QRPA matrix elements $A_{pn,p'n'}$ and $B_{pn,p'n'}$. We can easily do this by rewriting the operator $\vec{\tau}\cdot\vec{\tau}'$ in that equation in terms of the operators "1" and $P_\tau\equiv\frac{1}{2}(1+\vec{\tau}\cdot\vec{\tau}')$ and then keeping only the terms that contain P_τ. Finally, we modify the part of the code that treats pairing so that it can separately produce isovector ($S=0$) and isoscalar ($S=1$) matrix elements.

We adopt the Skyrme functional (or effective interaction) SkM* [38]; that functional has been shown to describe nuclear deformation well and reproduces low-lying quadrupole vibrations in rare-earth nuclei noticeably better than the comparably popular functional SLy4 [14]. We modify the time-odd particle-hole part of the functional as in Ref. [39], which discussed charge-changing transitions, by setting the parameters (defined in that reference) $C_1^T=0$, $C_1^{\nabla s}=0$, and $C_1^s[0]=C_1^s[\rho_{\rm nm}]=100$ Mev fm^3 ($\rho_{\rm nm}$ is the nuclear-matter density). With these modifications, the functional reproduces [19] the location of the Gamow-Teller resonance and the fraction of observable strength in the resonance. We will report results with and without the modifications to show their effect.

For the particle-particle part of the functional, we use a simple volume (zero-range) pairing interaction, the strength of which we adjust separately in the isoscalar channel ($T=0$) and in each of the three isovector ($T=1$ with $T_z=-1$, 0, and 1) channels. We describe the adjustment in more detail in the next section.

Evaluating the $0\nu\beta\beta$ matrix elements requires a multipole decomposition of $M'^{0\nu}$, suitable for cylindrical geometry. The details of that appear in the Appendix.

III. COMPUTATIONAL IMPLEMENTATION

Only recently have fully self-consistent deformed Skyrme-QRPA calculations entered the scene. The combination of methods we use here requires many thousands of CPU hours. Our methodology will, at some point, be obsolete because of the development of much faster finite amplitude [40] and

[1] This matrix element differs from the unprimed $M^{0\nu}$ used elsewhere by a factor of $g_A^2/1.25^2$. The two are equivalent when g_A is taken to be 1.25 but differ when it is modified. (Actually [30], g_A is closer to 1.27 than 1.25, but we follow tradition here.) The convention we use sets all the g_A dependences in the matrix element and none in the phase-space factor.

iterative Arnoldi [41] approaches, which use mean-field codes with time-independent constraints to solve the QRPA equations. Our method, by contrast, involves the explicit construction and diagonalization of the QRPA Hamiltonian matrix in a basis of two-canonical-quasiparticle states. These states are obtained from the HFB calculation mentioned previously.

To solve the initial HFB equations, we use the Vanderbilt deformed HFB code [42], which represents wave functions in a basis of B splines. Our cylindrical box has dimensions $r_{\max} = z_{\max} = 20$ fm, about three times as large as the radius of the heaviest nucleus studied here and a number found suitable in Ref. [42]. Our mesh spacing is 0.7 fm, and the energy cutoff of the HFB solutions is 60 MeV. We do not restrict the deformation (except to be axially symmetric) but rather allow the mean field to evolve freely to the nearest local binding-energy minimum. By using a range of quadrupole deformation parameters β_2 as initial guesses, we find one or more local minima and select the most bound solution as the mean field on which we base the QRPA. In ^{76}Ge, however, we do not use the most bound solution; we discuss the reasons for this exception in the next section. To obtain the strength of the proton-proton and neutron-neutron ($T = 1$, $T_z = \pm 1$) pairing interaction, we match the HFB pairing gaps with the experimental pairing gaps obtained from a three-point interpolation formula with separation energies from the evaluated nuclear structure data file (ENSDF) [43] database.

The computational requirements for running our charge-changing QRPA code are significantly less than those for the like-particle code on which it is based because (a) the proton-neutron two-quasiparticle basis is only about half the size of the like-two-quasiparticle basis, and (b) the removal of the Coulomb interaction relieves us of a large computational burden. For a given multipole, our charge-changing code typically runs much faster than the like-particle code. That speedup, however, still leaves us with runs that consume many thousands of CPU hours per multipole in each nucleus.

We cannot include all one-quasiproton–one-quasineutron states in our QRPA basis and so truncate the same way as in Ref. [14]. The truncation is controlled by two parameters $v_{\rm cut}^{\rm pp}$ and $v_{\rm cut}^{\rm ph}$. The first allows us to remove two-quasiparticle states with almost completely two-particle or two-hole nature (i.e., states that primarily lie in the $A \pm 2$ neighbors of the reference nucleus instead of the intermediate double-β nucleus), and the second lets us cut out states in which one of the particles is far below the Fermi surface and the other is far above it. Such excitations have very high energy and do not mix significantly with lower-energy states. In practice, 15 000 two-quasiparticle states for the lowest multipoles, out of a total of about 500 000, are enough to approximate the exact answer very well, making the construction and diagonalization of the QRPA matrix tractable on a supercomputer.

After diagonalizing the QRPA Hamiltonian, we need to determine the double-β-decay matrix elements. For $0\nu\beta\beta$ decay, the matrix element can be written as

$$M'^{0\nu} = \frac{2R}{(1.25)^2\pi} \sum_{pn} \langle 0_f^+ | c_{-p}^\dagger c_n | N \rangle \sum_{NN'} \langle N | N' \rangle \times \sum_{p'n'} \langle N' | c_{p'}^\dagger c_{-n'} | 0_i^+ \rangle \left(K^F_{pn,p'n'} + K^{\rm GT}_{pn,p'n'} \right), \quad (7)$$

where the $c_k^\dagger$ are particle-creation operators, the indices with p refer to protons and those with n to neutrons, each index stands for the set of quantum numbers $p = \{j_p^z, \pi_p, k_p\}$ (angular momentum along the intrinsic axis, parity, and an additional enumerating index), a minus sign in front of an index means that the sign of the j^z quantum number is reversed, and

$$K^F_{pn,p'n'} = \int_0^\infty q\, dq\, \langle pp' | \frac{j_0(qr_{12}) h_F(q)}{q + \overline{E} - (E_i + E_f)/2} \tau_1^+ \tau_2^+ | nn' \rangle ,$$
$$K^{\rm GT}_{pn,p'n'} = \int_0^\infty q\, dq\, \langle pp' | \frac{j_0(qr_{12}) h_{\rm GT}(q) \vec{\sigma}_1 \cdot \vec{\sigma}_2}{q + \overline{E} - (E_i + E_f)/2} \tau_1^+ \tau_2^+ | nn' \rangle . \quad (8)$$

The two-particle states in Eq. (8) are antisymmetrized. We use a multipole expansion, detailed in the Appendix, and B-spline integration to evaluate the two-body matrix elements in Eq. (8). The coding for the two-neutrino two-body matrix elements, which we use to evaluate the matrix element in Eq. (6), requires no Bessel function expansion.

Two-neutrino decay is simpler for another reason as well; only states with angular momentum and parity $J^\pi = 1^+$ contribute to the matrix element. In our deformed calculation, we follow the usual procedure [4,44] for representing laboratory states in a rigid-rotor approximation as combinations of (a) Wigner functions D^J_{MK} and D^J_{M-K} of Euler angles, and (b) an intrinsic QRPA state with a well-defined projection K of the angular momentum J along the symmetry axis. $M^{2\nu}$, thus, gets contributions only from states with $|K| \leqslant 1$. In neutrinoless decay, on the other hand, states with any K^π contribute. The contributions get progressively smaller as K gets larger. Including states with $|K| \leqslant 10$ is enough to approximate the matrix element accurately as Fig. 1 shows.

One interesting feature of Eq. (7) is the presence of the overlap $\langle N | N' \rangle$. The QRPA is a small-amplitude approximation, and although it provides transition densities from a ground state to excited states, it cannot, without extension, provide excited-state wave functions. The excited states $|N\rangle$ and $|N'\rangle$ are based on different quasiparticle vacua, and the quasiboson approximation that is inherent in the QRPA erases the information necessary to relate the two vacua. Two

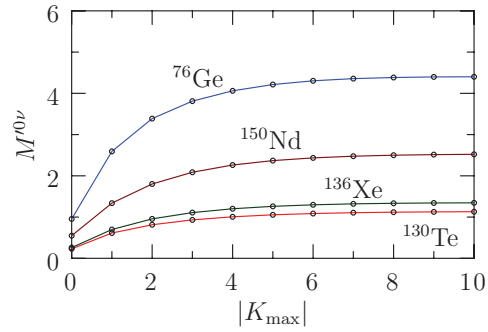

FIG. 1. (Color online) The cumulative $0\nu\beta\beta$ matrix elements (which uses SkM* and $g_A = 1.0$) as the number of intermediate-state multipoles K^π is increased. Convergence is reached by $|K| = 10$. Both positive and negative parities are included as are both Fermi and Gamow-Teller contributions.

expressions for the overlap have been given in the past few years: one, from Ref. [5], neglects "scattering terms" even though they cannot be shown to be small, and the other, laid out in Ref. [45], uses the form of the boson vacuum but replaces the bosons with the fermion pairs from which they stem. Unfortunately, this last idea leads to expressions that can only be evaluated perturbatively; these become unwieldy after the lowest couple of orders in the expansion, the convergence of which may not be fast. Here, we simply evaluate the overlap in the quasi-Tamm-Dancoff approximation (QTDA) (by neglecting the QRPA "Y" amplitudes); in this limit of the QRPA, excited states are well-defined two-quasiparticle excitations of HFB vacua and require no bosonization. The results are not very different from those obtained in the scheme proposed in Ref. [5]. We provide more details in the Appendix.

As is typical in QRPA calculations, we use the measured values of two-neutrino decay rates to fit proton-neutron pairing strengths (which have no effect in the HFB part of the calculation because of the significant neutron excess). By following a suggestion in Ref. [46], we adjust the isovector ($T = 1$, $T_z = 0$) strength so that the Fermi $2\nu\beta\beta$ matrix element vanishes as it should (almost) because the ground state of the final nucleus has a different isospin than does the double-isobar-analog state of the initial nucleus. If, instead, we fix the proton-neutron isovector pairing strength at the average of the proton-proton and neutron-neutron pairing strengths, we find a nearly identical result. The isoscalar pairing strength, which here we call V_0, is the parameter typically called g_{pp} in other QRPA calculations. We adjust it so as to reproduce the experimental two-neutrino matrix element with both an unquenched ($g_A = 1.25$, see the footnote) and a quenched ($g_A = 1.0$) axial-vector coupling constant. We then use the resulting pairing strengths in computing the $0\nu\beta\beta$ matrix elements, once for each value of g_A. For ^{130}Te and ^{136}Xe, we compute the neutrinoless double-β-decay matrix element with the unmodified SkM* over a range of isoscalar pairing values V_0 to assess its sensitivity to the fit. Some other authors (e.g. in Ref. [47]) renormalize the QRPA so that the effects of proton-neutron pairing are weakened; that procedure would spoil the self-consistency of the HFB-QRPA framework, and we do not adopt it here.

IV. RESULTS AND DISCUSSION

We start by comparing the quadrupole deformation parameters β_2 obtained from our HFB calculation to other theoretical and experimental values in Table I. With the exception of ^{76}Se where our Skyrme-HFB computation fails to converge to a solution with significant deformation, our quadrupole deformations are similar to those obtained by using the Sk3 and SG2 Skyrme interactions in Ref. [9]. The failure is most likely due to a very flat bottom of the binding-energy curve with respect to deformation in ^{76}Se.

In ^{76}Ge, the minimum energy occurs at a prolate deformation of $\beta_2 = 0.18$. This deformation is so different from that of ^{76}Se, however, that our predicted two-neutrino matrix element is smaller than the measured value no matter what we use for g_A or V_0. We, therefore, choose to use the local near-spherical minimum ($\beta_2 = -0.025$) for ^{76}Ge instead. As we will see, this gives us a result that is not too different from other QRPA numbers, including those of Ref. [6], which presents both spherical-spherical and prolate-prolate calculations. It also indicates, however, that the QRPA is inadequate in this system. The soft surfaces with multiple minima require a formulation that mixes mean fields, e.g., the generator-coordinate method [a part of what is now often referred to as energy-density functional (EDF) theory] of Ref. [50] or an extension thereof.

TABLE I. The quadrupole deformations β_2 of the initial and final nuclei in our paper, compared with the values obtained in Ref. [9] and experimental values from Refs. [48,49].

		Ref. [9]		Expt.	
	This paper	Sk3	SG2	Ref. [48]	Ref. [49]
^{76}Ge	0.184[a]	0.161	0.157	0.095(30)	0.2623(9)
^{76}Se	−0.018	−0.181	−0.191	0.163(33)	0.3090(37)
^{130}Te	0.01	−0.076	−0.039	0.035(23)	0.1184(14)
^{130}Xe	0.13	0.108	0.161		0.1837(49)
^{136}Xe	0.004	0.001	0.016		0.122(10)
^{136}Ba	−0.021	0.009	0.070		0.1258(12)
^{150}Nd	0.27	0.266	0.271	0.367(86)	0.2853(21)
^{150}Sm	0.22	0.207	0.203	0.230(30)	0.1931(21)

[a]A value of −0.025 was used.

In the daughter nucleus ^{130}Xe, we get a prolate solution, which makes ours a QRPA calculation that takes the deformation into account in the decay of ^{130}Te. The study in Ref. [51], which uses HFB with the Gogny interaction, finds a second minimum with oblate deformation and a barrier of only 1 MeV or so that separates the two minima. As in ^{76}Se, therefore, the use of a single mean field in the construction of the ^{130}Xe ground state is somewhat suspect.

We do not reproduce experimental Q values as well as deformations, in part, because the errors in the binding energies of the nuclei add in quadrature. But for the record, our HFB calculation produces $Q = 4.84$ MeV (vs the experimental value of 2.04 MeV) in ^{76}Ge, $Q = 4.22$ MeV (vs the experimental value of 2.53 MeV) in ^{130}Te, $Q = 5.60$ MeV (vs 2.46 MeV) in ^{136}Xe, and $Q = 2.35$ MeV (vs 3.371 MeV) in ^{150}Nd. Other calculations with different Skyrme functionals produce discrepancies of the same order [52].

We turn now to the matrix elements themselves. Figure 2 displays the dependence of the $2\nu\beta\beta$ matrix element on the isoscalar pairing strength V_0 in the four systems we study. We use the recent evaluation of the phase-space factors in Ref. [29] to extract the experimental matrix elements. Because $M^{2\nu}$ for ^{136}Xe was recently measured for the first time by the EXO-200 [53] and KamLAND-Zen [24] groups, our QRPA double-β computation fits the strength of isoscalar pairing to the experimental matrix element rather than to the upper limit used, e.g., in Refs. [35,55].

Figure 3 illustrates the dependence of the $0\nu\beta\beta$ decay matrix element on V_0. The neutrinoless matrix element is less sensitive to this pairing mode than the two-neutrino matrix element. We collect our final results for the $0\nu\beta\beta$ matrix elements with both $g_A = 1.25$ and $g_A = 1.0$ in Table II. The modification of SkM* usually suppresses the $0\nu\beta\beta$ matrix

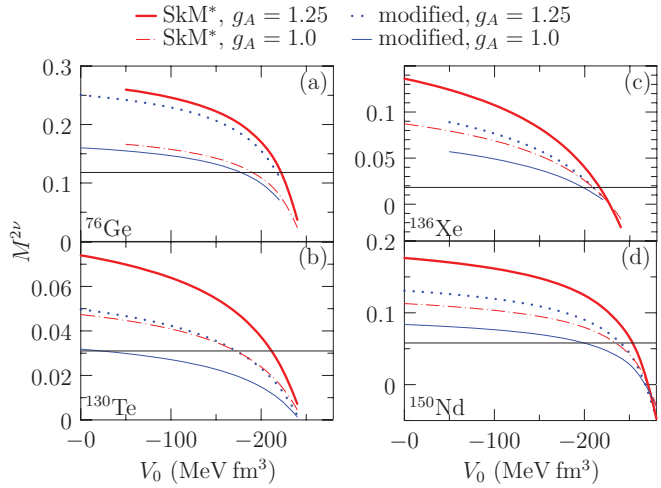

FIG. 2. (Color online) The dependence of two-neutrino double-β decay matrix elements on V_0, the isoscalar pairing strength. The thick solid and dashed (red) curves are produced by the original SkM* interaction, and the dotted and thin (blue) curves are produced by the modified interaction. The thick solid and dotted curves are computed with $g_A = 1.25$, and the dashed and thin solid curves are computed with the quenched value $g_A = 1.0$.

element by up to 15%. It actually seems to increase the matrix element in ^{130}Te by 17% for $g_A = 1.0$, but as Fig. 2 shows, the fitting procedure for V_0 with $g_A = 1.0$ gives an anomalously small value, and so that result must be taken with a grain of salt. In Table III, we compare our values with the modified SkM* and $g_A = 1.25$ with earlier theoretical results. Our matrix elements for ^{76}Ge and ^{150}Nd are in good agreement with the spherical result for Ge and the deformed one for Nd in Ref. [6]. For ^{136}Xe and ^{130}Te, we get noticeably smaller matrix elements than obtained in prior papers, all of which used the spherical

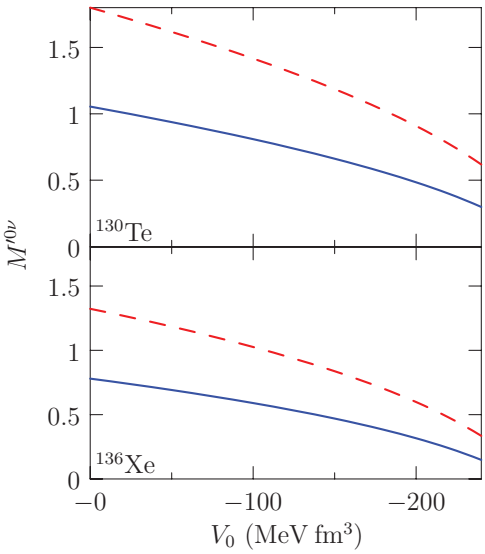

FIG. 3. (Color online) The dependence of $M^{0\nu}$ in ^{136}Xe and ^{130}Te on the V_0 produced by the unmodified SkM* interaction. The solid curve represents the results with $g_A = 1.0$, and the dashed curve represents the results with $g_A = 1.25$.

TABLE II. The $0\nu\beta\beta$ matrix elements in our Skyrme-HFB-QRPA calculation with both the functional SkM* and a modified version of it and with both a quenched and an unquenched axial-vector coupling constant g_A.

	SkM*		Modified SkM*	
	$g_A = 1.0$	$g_A = 1.25$	$g_A = 1.0$	$g_A = 1.25$
^{76}Ge	4.40	5.53	4.12	5.09
^{130}Te	1.13	1.38	1.32	1.37
^{136}Xe	1.26	1.68	1.18	1.55
^{150}Nd	2.52	3.14	2.14	2.71

QRPA. Figure 4 graphically displays the same information as the table.

The suppression we see in ^{130}Te can be attributed to the deformation of the daughter nucleus. Previous QRPA calculations for ^{130}Te [35,55] have assumed spherical symmetry. We have already mentioned, however, that a single minimum may not be adequate to represent the ground state of ^{130}Xe. We suspect that the complete neglect of deformation in previous papers leads to a matrix element that is too large but it may also be that our sharp prolate Xe ground state yields one that is too small.

The other decay in which we disagree significantly with previous QRPA calculations is that of ^{136}Xe. Our significantly smaller result, here, is not caused by deformation difference, nor does it come from the availability of new two-neutrino-decay data. Instead, it can be traced to the overlap between the initial and the final HFB mean fields. This overlap usually reflects the difference in deformation between the mother and the daughter nuclei and, for that reason, has been completely neglected in previous QRPA calculations for the decay of ^{136}Xe where both the initial and the final nuclei are spherical. We find here, however, that differences in pairing structure in the neutron mean fields lead to a small overlap: $\langle \mathrm{HFB}_f | \mathrm{HFB}_i \rangle = 0.47$. The suppression is related to the $N = 82$ shell closure, which produces a sharp Fermi surface that smooths measurably with the addition of two neutrons. We see no reason to completely neglect the overlap, but the situation may be analogous to that in the decay of ^{130}Te. A more realistic representation of pairing than is offered by the HFB mean field might make the difference in structure between the initial and the final nuclei a little less dramatic.

TABLE III. Comparison of our $0\nu\beta\beta$ matrix elements from the modified SkM* functional and $g_A = 1.25$ with those obtained from the interacting shell model (ISM, [54]), QRPA calculations by the Tübingen group [6,35] (QRPA/T) and Jyväskylä group [55] (QRPA/J), the EDF method [50], projected HFB [56] (PHFB), and the interacting boson model [57] (IBM-2). Prior results that include deformation are indicated by asterisks.

	Present paper	QRPA/T	QRPA/J	ISM	IBM-2	PHFB	EDF
^{76}Ge	5.09	5.30, 4.69*	5.355	2.96	5.465		4.60
^{130}Te	1.37	4.92	4.221	2.81	4.059	4.66	5.13
^{136}Xe	1.55	3.11	2.802	2.32	2.220		4.20
^{150}Nd	2.71	3.34*			2.321	3.24	1.71

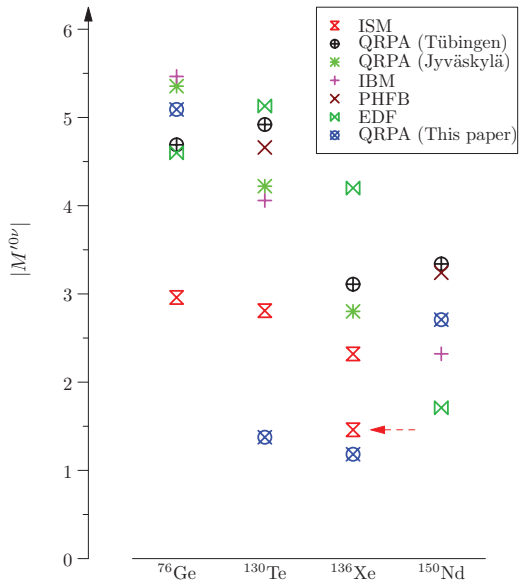

FIG. 4. (Color online) The results of Table III for $g_A = 1.25$. The dashed (red) arrow points to the new shell-model result of Ref. [58] in ^{136}Xe.

Interestingly, a recent shell-model [58] calculation finds that by increasing the model-space size produces the smallest matrix element yet for this decay: 1.46.

All the substantial differences between our QRPA calculations and others can be traced to deformation or pairing effects that were neglected in previous papers. Our use of a self-consistent QRPA with all nucleons treated as active participants, the continuum accounted for, etc., does not, in itself, change results dramatically. That finding is not altogether surprising. Self-consistency is important in the QRPA partly because it eliminates spurious strength. In the charge-changing QRPA, however, the absence of proton-neutron mixing in the HFB and the explicit breaking of the isospin mean that there is no spurious strength even in non-self-consistent calculations. More importantly, it is already well known [59] that differences between variants of the QRPA largely disappear when the strength of the isoscalar pairing interaction is adjusted so that each variant reproduces the measured two-neutrino rate. Our variant does not escape this fate; that one parameter is like a broad and coarse brush that paints over any sophistication in the underlying method.

V. CONCLUSIONS

We have performed large-scale Skyrme-HFB-QRPA computations for four important double-β emitters. We have allowed for axial deformation of the initial and final nuclei. Our implementation increases the scale of the computation to the limits of contemporary technology.

For ^{76}Ge and the very deformed ^{150}Nd, our results are in line with the earlier results of Ref. [6]. We note, however, that the assumption, both here and elsewhere, that the ^{76}Ge and ^{76}Se ground states are spherical probably results in a matrix element that is too large.

In ^{130}Te, we improve on the ground state used in previous QRPA calculations by taking into account the deformation of the final nucleus. Shape coexistence in the daughter ^{130}Xe is beyond the scope of the QRPA; however, if present, it could further modify the value of the matrix element.

Our calculation in ^{136}Xe is among the first in that nucleus to incorporate the recent two-neutrino-decay measurements. And we know of no other in ^{136}Xe that takes into account the overlap of the two sets of QRPA intermediate states. The overlap is smaller than one might expect because of the sharp neutron Fermi surface in the initial nucleus. In reality, the Fermi surface cannot be perfectly sharp, and the true matrix element is probably not suppressed quite this much. The recent shell-model result for this matrix element [58], however, implies that past computations may have overestimated the ^{136}Xe double-β-decay rate.

Our computation demonstrates that there is little to be gained by further increasing the size and sophistication of QRPA calculations. Any straightforward alterations to the QRPA, other than the development of a better energy-density functional, are unlikely to substantially improve the results. We have reached the point at which shortcomings of the QRPA itself restrict improvement. The inability to treat shape coexistence is an issue, at least, for the daughter nuclei ^{76}Se and ^{130}Xe. The mean-field treatment of pairing may be a problem in nuclei, such as ^{136}Xe, that have closed shells. We can address these issues only by moving beyond the QRPA.

ACKNOWLEDGMENTS

Support for this work was provided through the Scientific Discovery through Advanced Computing (SciDAC) program funded by the US Department of Energy, Office of Science, Advanced Scientific Computing Research and Nuclear Physics, under Award No. DE-SC0008641, and by the UNEDF SciDAC Collaboration under DOE Grants No. DE-FC02-07ER41457 and No. DE-FC02-09ER41584. One of us (M.T.M.) gratefully acknowledges fruitful discussions with Professor M. Horoi, alongside the support and hospitality he extended at Central Michigan University during the spring of 2012. This work used the Extreme Science and Engineering Discovery Environment (XSEDE), which is supported by National Science Foundation Grant No. OCI-1053575. Most of the computations were performed on Kraken at the National Institute for Computational Sciences (http://www.nics.tennessee.edu/). This research also used resources of the National Energy Research Scientific Computing Center, which is supported by the Office of Science of the US Department of Energy under Contract No. DE-AC02-05CH11231.

APPENDIX: NEUTRINOLESS DOUBLE-β-DECAY MATRIX ELEMENTS IN THE CYLINDRICAL BOX

Equation (7) is, in essence, a trace of a product of four large square matrices. The transition densities in that equation are

$$\langle 0_f^+ | c_{-p}^\dagger c_n | N \rangle = s_p v_p u_n X_{pn}^N + u_p s_n v_n Y_{-p-n}^N, \qquad \text{(A1)}$$

and

$$\langle N'|c^\dagger_{p'}c_{-n'}|0^+_i\rangle = -u_{p'}s_{n'}v_{n'}X^{N'}_{p'n'} - s_{p'}v_{p'}u_{n'}Y^{N'}_{-p'-n'}. \quad \text{(A2)}$$

Here, the indices p and p' indicate protons, and n and n' indicate neutrons as discussed in the main text; $c^\dagger_p$ is a proton creation operator, and u_p and s_pv_p are the proton occupation amplitudes in the canonical basis in the notation of Ref. [44]. X^N_{pn} and Y^N_{-p-n} are forward-going and backward-going QRPA amplitudes.

To reduce the number of nested numerical integrals in the $0\nu\beta\beta$ matrix elements in Eq. (7), we take advantage of the following expansion for the spherical Bessel function in Eq. (8):

$$j_0(qr_{ab}) = 4\pi\sum_{l=0}^{\infty} j_l(qr_a)j_l(qr_b)\sum_{m=-l}^{l} Y^*_{lm}(\hat{r}_a)Y_{lm}(\hat{r}_b). \quad \text{(A3)}$$

This allows us to separate the integrals over coordinates of the two nucleons,

$$K^F_{pn,p'n'} = \int_0^\infty dq\,\frac{qh_F(q^2)}{q+E_{\rm ave}}\sum_{l=K}^{\infty}(2l+1) \times\frac{(l-K)!}{(l+K)!}I^{lK}_{-pn}(q)I^{lK}_{p'-n'}(q), \quad \text{(A4)}$$

and

$$K^{\rm GT}_{pn,p'n'} = \int_0^\infty dq\,\frac{qh_{\rm GT}(q^2)}{q+E_{\rm ave}}\sum_{\mu=-1}^{1}(-1)^\mu \times\sum_{l=\max(0,K-\mu)}^{\infty}(2l+1)\frac{[l-(K-\mu)]!}{[l+(K-\mu)]!} \times I^{l,K-\mu,-\mu}_{-pn}(q)I^{l,K-\mu,\mu}_{p'-n'}(q), \quad \text{(A5)}$$

where $E_{\rm ave} = \bar{E} - (E_i+E_f)/2$. Naturally, the infinite summations over l must be truncated. For most values of the neutrino energy q, not many terms are needed for convergence. In the program, we truncate the expansion dynamically by requiring a preset accuracy in the quadrature for each value of q.

The axial symmetry of the normalized canonical single-particle wave functions means that they can be written in the form

$$\Psi_a(\vec{r}) = \frac{1}{\sqrt{2\pi}}\sum_{s=\pm1/2}\psi_a(s;\rho,z)e^{i(j^z_a-s)\phi}\chi_s, \quad \text{(A6)}$$

where s is the spin projection, χ_s is a standard two-component spinor, and j^z_a is the angular momentum projection onto the intrinsic axis. The integrations over the azimuthal angle ϕ are trivial, and the integrals $I^{lm}_{ab}(q)$ and $I^{lmv}_{ab}(q)$ are, therefore, only two dimensional,

$$I^{lm}_{ab}(q) = \int_{-\infty}^{\infty}dz\int_0^\infty d\rho\,\rho\psi^\dagger_a(\rho,z)\psi_b(\rho,z) \times j_l(q\sqrt{\rho^2+z^2})P^m_l\left(\frac{z}{\sqrt{\rho^2+z^2}}\right), \quad \text{(A7)}$$

and

$$I^{lmv}_{ab}(q) = \int_{-\infty}^{\infty}dz\int_0^\infty d\rho\,\rho\psi^\dagger_a(\rho,z)\sigma_v\psi_b(\rho,z) \times j_l(q\sqrt{\rho^2+z^2})P^m_l\left(\frac{z}{\sqrt{\rho^2+z^2}}\right). \quad \text{(A8)}$$

Here, the $P^m_l(x)$ are the usual associated Legendre polynomials, σ_v are the Pauli matrices in the spherical vector basis, and

$$\psi_a(\rho,z) = \begin{pmatrix}\psi_a(+1/2;\rho,z)\\ \psi_a(-1/2;\rho,z)\end{pmatrix}. \quad \text{(A9)}$$

As discussed in the main body of the text, we also need to evaluate the overlaps $\langle N|N'\rangle$ between the QRPA states that stem from different mean fields. A satisfactory expression for these is lacking, but the chief ingredient in any such expression will be the overlap of two HFB vacua. The generalized Thouless theorem [44] that relates the two nonorthogonal quasiparticle vacua $|{\rm HFB}_i\rangle$ (initial state) and $|{\rm HFB}_f\rangle$ (final state) to each other is as follows:

$$|{\rm HFB}_i\rangle = \mathcal{N}^{-1}\exp\left(\sum_{kl}D_{kl}a^{(f)\dagger}_k a^{(f)\dagger}_l\right)|{\rm HFB}_f\rangle, \quad \text{(A10)}$$

where the $a^{(f)\dagger}_k$'s are quasiparticle creation operators in the final nucleus. The normalization factor is related to the transformation coefficients D_{kl} via the Onishi formula,

$$\mathcal{N} = \langle{\rm HFB}_f|{\rm HFB}_i\rangle^{-1} = \sqrt{\det(1+D^\dagger D)}. \quad \text{(A11)}$$

Because the canonical-basis wave functions form a complete set, there exists a linear transformation between the two HFB solutions,

$$a^{(f)\dagger}_k = \sum_n\left(\mathcal{R}_{kn}a^{(i)\dagger}_n + \mathcal{S}_{k,-n}a^{(i)}_{-n}\right), \quad \text{(A12)}$$

where

$$\mathcal{R}_{kn} = \langle n|k\rangle(u_ku_n + s_kv_ks_nv_n), \quad \text{(A13)}$$

and

$$\mathcal{S}_{k,-n} = \langle n|k\rangle(u_ks_nv_n - s_kv_ku_n). \quad \text{(A14)}$$

By substituting Eqs. (A10) and (A12) into the definition of the quasiparticle vacuum,

$$a^{(f)}_{-k}|{\rm HFB}_f\rangle = 0, \quad \text{(A15)}$$

by expanding the exponential, and by comparing the terms that contain one quasiparticle creation operator, we get the matrix equation,

$$\mathcal{R}^*D = -\mathcal{S}^*, \quad \text{(A16)}$$

from which we can obtain the transformation coefficients D_{kl}.

As mentioned earlier, we approximate the QRPA overlaps by QTDA overlaps, i.e., by neglecting the Y's. This finally leads to the expression,

$$\langle N|N'\rangle = \mathcal{N}^{-1} \sum_{pn} \sum_{p'n'} X^{N*}_{pn} X^{N'}_{p'n'} \left(\mathcal{R}_{p'p} + \sum_{p''} \mathcal{S}_{p'p''} D_{p''p} \right) \times \left(\mathcal{R}_{n'n} + \sum_{n''} \mathcal{S}_{n'n''} D_{n''n} \right). \quad \text{(A17)}$$

This formula differs slightly from the one presented in Ref. [5] and used in most QRPA double-β-decay calculations. Our overlap differs in that we keep the transformation between the two HFB bases accurate and neglect the usually tiny term proportional to two Y amplitudes. In test calculations, we find the numerical difference between the two prescriptions to be negligible as the common leading term is already a good approximation. A more consistent evaluation of these overlaps that includes ground-state correlations can easily get both very complicated and computationally demanding, as recent work in the like-particle QRPA [45] shows.

[1] F. T. Avignone III, S. R. Elliott, and J. Engel, Rev. Mod. Phys. **80**, 481 (2008).
[2] J. D. Vergados, H. Ejiri, and F. Šimkovic, Rep. Prog. Phys. **75**, 106301 (2012).
[3] A. S. Barabash, J. Phys. G **39**, 085103 (2012).
[4] M. S. Yousef, V. Rodin, A. Faessler, and F. Šimkovic, Phys. Rev. C **79**, 014314 (2009).
[5] F. Šimkovic, L. Pacearescu, and A. Faessler, Nucl. Phys. A **733**, 321 (2004).
[6] D.-L. Fang, A. Faessler, V. Rodin, and F. Šimkovic, Phys. Rev. C **83**, 034320 (2011).
[7] O. Moreno, R. Álvarez-Rodríguez, P. Sarriguren, E. M. de Guerra, F. Šimkovic, and A. Faessler, J. Phys. G **36**, 015106 (2009).
[8] O. Moreno, R. Álvarez-Rodríguez, P. Sarriguren, E. M. de Guerra, J. M. Udías, and J. R. Vignote, Phys. Rev. C **74**, 054308 (2006).
[9] R. Álvarez-Rodríguez, P. Sarriguren, E. M. de Guerra, L. Pacearescu, A. Faessler, and F. Šimkovic, Phys. Rev. C **70**, 064309 (2004).
[10] L. Pacearescu, V. Rodin, F. Šimkovic, and A. Faessler, Phys. Rev. C **68**, 064310 (2003).
[11] A. Bobyk, W. A. Kamiński, and F. Šimkovic, Phys. Rev. C **63**, 051301R (2001).
[12] M. Cheoun, A. Bobyk, A. Faessler, F. Sĭmkovic, and G. Teneva, Nucl. Phys. A **564**, 329 (1993).
[13] C. De Conti, F. Krmpotić, and B. V. Carlson, arXiv:1202.3511.
[14] J. Terasaki and J. Engel, Phys. Rev. C **82**, 034326 (2010).
[15] J. Terasaki and J. Engel, Phys. Rev. C **84**, 014332 (2011).
[16] K. Yoshida and T. Nakatsukasa, Phys. Rev. C **83**, 021304(R) (2011).
[17] S. Péru, G. Gosselin, M. Martini, M. Dupuis, S. Hilaire, and J.-C. Devaux, Phys. Rev. C **83**, 014314 (2011).
[18] K. Yoshida and N. Van Giai, Phys. Rev. C **78**, 064316 (2008).
[19] T. Shafer and J. Engel (unpublished).
[20] F. Bellini *et al.*, Astropart. Phys. **33**, 169 (2010).
[21] The GERDA Collaboration, M. Agostini *et al.*, J. Phys. G **40**, 035110 (2013).
[22] D. G. Phillips II *et al.*, J. Phys.: Conf. Ser. **381**, 012044 (2012).
[23] M. Auger *et al.* (The EXO Collaboration), Phys. Rev. Lett. **109**, 032505 (2012).
[24] A. Gando *et al.* (KamLAND-Zen Collaboration), Phys. Rev. C **85**, 045504 (2012).
[25] H. Ohsumi, J. Phys.: Conf. Ser. **120**, 052054 (2008).
[26] C. Kraus and S. J. M. Peeters, Prog. Part. Nucl. Phys. **64**, 273 (2010).
[27] F. Sánchez, Nucl. Phys. B, Proc. Suppl. **198**, 71 (2009).
[28] N. Ishihara, T. Ohama, and Y. Yamada, Nucl. Instrum. Methods Phys. Res. A **373**, 32 (1996).
[29] J. Kotila and F. Iachello, Phys. Rev. C **85**, 034316 (2012).
[30] Particle Data Group, J. Beringer *et al.*, Phys. Rev. D **86**, 010001 (2012).
[31] G. Pantis and J. Vergados, Phys. Lett. B **242**, 1 (1990).
[32] W. C. Haxton and G. J. Stephenson, Jr., Prog. Part. Nucl. Phys. **12**, 409 (1984).
[33] O. Civitarese and J. Suhonen, Nucl. Phys. A **607**, 152 (1996).
[34] F. Šimkovic, Czech J. Phys. B **38**, 371 (1988).
[35] F. Šimkovic, A. Faessler, H. Müther, V. Rodin, and M. Stauf, Phys. Rev. C **79**, 055501 (2009).
[36] J. Engel and G. Hagen, Phys. Rev. C **79**, 064317 (2009).
[37] J. Terasaki, J. Engel, M. Bender, J. Dobaczewski, W. Nazarewicz, and M. Stoitsov, Phys. Rev. C **71**, 034310 (2005).
[38] J. Bartel, P. Quentin, M. Brack, C. Guet, and H.-B. Håkansson, Nucl. Phys. A **386**, 79 (1982).
[39] M. Bender, J. Dobaczewski, J. Engel, and W. Nazarewicz, Phys. Rev. C **65**, 054322 (2002).
[40] P. Avogadro and T. Nakatsukasa, Phys. Rev. C **84**, 014314 (2011).
[41] J. Toivanen, B. G. Carlsson, J. Dobaczewski, K. Mizuyama, R. R. Rodríguez-Guzmán, P. Toivanen, and P. Veselý, Phys. Rev. C **81**, 034312 (2010).
[42] E. Terán, V. E. Oberacker, and A. S. Umar, Phys. Rev. C **67**, 064314 (2003).
[43] "Evaluated Nuclear Structure Data File (ENSDF)", http://www.nndc.bnl.gov/ensdf/.
[44] P. Ring and P. Schuck, *The Nuclear Many-Body Problem*, Texts and Monographs in Physics (Springer, Berlin, 2004).
[45] J. Terasaki, Phys. Rev. C **86**, 021301(R) (2012).
[46] V. Rodin and A. Faessler, Phys. Rev. C **84**, 014322 (2011).
[47] J. Schwieger, F. Šimkovic, and A. Faessler, Nucl. Phys. A **600**, 179 (1996).
[48] G. A. Lalazissis, S. Raman, and P. Ring, At. Data Nucl. Data Tables **71**, 1 (1999).
[49] S. Raman, C. W. Nestor, Jr., and P. Tikkanen, At. Data Nucl. Data Tables **78**, 1 (2001).
[50] T. R. Rodríguez and G. Martínez-Pinedo, Phys. Rev. Lett. **105**, 252503 (2010).
[51] L. M. Robledo, R. R. Rodríguez-Guzmán, and P. Sarriguren, Phys. Rev. C **78**, 034314 (2008).
[52] J. Dobaczewski, M. Stoitsov, and W. Nazarewicz, in *Skyrme-HFB Deformed Nuclear Mass Table*, edited by R. Bijker, A. Frank, and R. F. Casten, AIP Conf. Proc. No. 726 (AIP, New York, 2004), p. 51.

[53] N. Ackerman *et al.* (The EXO Collaboration), Phys. Rev. Lett. **107**, 212501 (2011).
[54] J. Menéndez, A. Poves, E. Caurier, and F. Nowacki, Nucl. Phys. A **818**, 139 (2009).
[55] J. Suhonen and M. Kortelainen, Int. J. Mod. Phys. E **17**, 1 (2008).
[56] P. K. Rath, R. Chandra, K. Chaturvedi, P. K. Raina, and J. G. Hirsch, Phys. Rev. C **82**, 064310 (2010).
[57] J. Barea and F. Iachello, Phys. Rev. C **79**, 044301 (2009).
[58] M. Horoi and B. A. Brown, arXiv:1301.0256.
[59] V. A. Rodin, A. Faessler, F. Šimkovic, and P. Vogel, Phys. Rev. C **68**, 044302 (2003).